

Nb₆I₁₁, DNb₆I₁₁, and HNb₆I₁₁: A Powder Neutron Diffraction and Inelastic Scattering Study †

Andrew N. Fitch, S. Andrew Barrett, and Brian E. F. Fender*
Inorganic Chemistry Laboratory, University of Oxford, Oxford OX1 3QR
 Arndt Simon
Max-Planck-Institut für Festkörperforschung, D-7000 Stuttgart 80, Germany

Powder neutron diffraction and inelastic scattering studies on DNb₆I₁₁ and HNb₆I₁₁ suggest that the interstitial hydrogen atom is displaced slightly from the centre of gravity of the surrounding Nb₆ cage in the low-symmetry phase. The inelastic scattering spectrum shows a broad peak for the Nb–H interactions at about 135 meV.

A feature of the inorganic chemistry of niobium, tantalum, molybdenum, and tungsten is the formation of octahedral metal atom clusters by the halides of low oxidation state.^{1–3} These halides contain either [M₆X₁₂]ⁿ⁺ units in which each edge of the octahedral metal cluster is bridged by halide atoms, or [M₆X₈]ⁿ⁺ units in which the halide is co-ordinated to each face of the metal clusters. The number of *d* electrons available determines the type of cluster which is formed as there are eight metal–metal bonding orbitals in the [M₆X₁₂]ⁿ⁺ units but 12 in the [M₆X₈]ⁿ⁺ units.⁴ There are numerous examples of each type: binary compounds with [M₆X₁₂]ⁿ⁺ units include Nb₆F₁₅,⁵ Nb₆Cl₁₄,⁶ Ta₆I₁₄,⁷ W₆Cl₁₈,⁸ Ta₆Cl₁₅,⁹ as well as the hydrates of various niobium and tantalum halides;¹⁰ [M₆X₈]ⁿ⁺ clusters are found in, for example, Mo₆Cl₁₂,¹¹ W₆Br₁₄,¹² Cs₂[Mo₆Cl₈]Cl₆,¹³ and Nb₆I₁₁.^{14–17}

The compound Nb₆I₁₁ is unusual, not only because it is alone amongst the Group 5 halides to adopt the [M₆X₈]³⁺ cluster, but also because each cluster has only 19 *d* electrons available for metal–metal bonding. It is believed that this apparent electron deficiency is closely related to the ability of Nb₆I₁₁ to absorb hydrogen to form HNb₆I₁₁,¹⁸ the compound investigated in the present paper. The number of electrons in bonding cluster orbitals is increased by one due to the hydrogen atom.^{19,20} In accordance with this idea, hydrogen absorption is also found with CsNb₆I₁₁ leading to CsHNb₆I₁₁,²¹ whereas Nb₆Cl₁₄ and Mo₆Cl₁₂, both compounds with completely filled metal–metal bonding *d* orbitals, do not take up hydrogen. Earlier results claiming the formation of H_{1.2}Nb₆Cl₁₄ and H_{0.66}Mo₆Cl₁₂²² had to be revised.²³

Both Nb₆I₁₁ and HNb₆I₁₁ undergo a second-order transition from a low-temperature form in the non-centrosymmetric space group *P2₁cn* to a high-temperature form in the higher symmetry centrosymmetric space group *Pccn*.²⁴ For Nb₆I₁₁, the structural transition is accompanied by a magnetic transition from a doublet to a quartet state, whereas for HNb₆I₁₁ a transition from a singlet to a triplet state is observed.²⁵ The change in symmetry occurs at 274 and 324 K respectively and has been fully characterized for the heavy atoms by single-crystal X-ray diffraction.¹⁷

Early powder neutron-diffraction studies of ¹HNb₆I₁₁ gave a strong indication that the hydrogen was incorporated into the cluster as an interstitial atom.¹⁸ In the high-temperature phase it is thought that the hydrogen atom is at the special crystallographic position 4a (0,0,0) at the centre of gravity of the Nb₆ octahedron, whereas below the transition temperature a displacement from this position is possible. In [N(PPh₃)₂][HCo(CO)₁₅], single-crystal neutron diffraction indicates the hydrogen atom to be at the geometric centre of the cluster²⁶ within experimental error, but in [HNi₁₂(CO)₂₁]³⁻ and

[H₂Ni₁₂(CO)₂₁]²⁻ (ref. 27) displacement towards one of the interior triangular faces of the octahedral cavities is observed.

In this study we use the relatively high coherent scattering cross-section of deuterium to probe more fully the position of the hydrogen atom within the [Nb₆I₈]³⁺ cluster in the low-temperature form by means of powder neutron diffraction. In addition, the high incoherent cross-section of the proton is used to highlight the vibrational characteristics of the bound hydrogen in neutron inelastic scattering measurements.

Experimental

The Nb₆I₁₁, HNb₆I₁₁, and DNb₆I₁₁ samples were prepared as described earlier¹⁸ by the reduction of Nb₃I₈ with niobium metal, followed by exposure to either gaseous H₂ or D₂ (assumed to be 99% isotopically pure) at 1 atm and 450 °C during 3 h. Deuterium was prepared by electrolysis of a solution of K₂CO₃ in D₂O of 99.7% purity.

Powder Neutron-diffraction Measurements.—The DNb₆I₁₁ sample (12 g) was contained in a silica tube and was examined at room temperature (295 K) on the PANDA diffractometer at AERE Harwell using a nominal wavelength of 2.41 Å. A germanium monochromator was used with a 90° take-off angle. Data were collected up to 2θ = 100° over 3 d. The counters arranged in three horizontal planes were employed.

Neutron Inelastic Scattering Measurements.—Neutron energy-loss measurements were made using the INIB beryllium filter spectrometer mounted on the hot source at the Institut Laue-Langevin, Grenoble. Measurements were made at room temperature over the energy range 50–300 meV for Nb₆I₁₁, HNb₆I₁₁, and DNb₆I₁₁ using the planes 200, 220, and 331 of copper to monochromate the incident beam.

Results and Discussion

DNb₆I₁₁: Powder Neutron Diffraction.—The powder neutron-diffraction pattern was analysed by the Rietveld method²⁸ with the following scattering lengths (10⁻¹² cm): D, 0.667; Nb, 0.705; I, 0.528; H, -0.374.²⁹ Several small peaks from β-NbD_x (*x* = 0.7, as judged by the values of the lattice parameters³⁰) as a minor impurity phase could be seen in the pattern overlapping with the peaks of the major phase DNb₆I₁₁. The exclusion of these regions would have resulted in the loss of over 40 reflections from the DNb₆I₁₁. We therefore made use of the program described by Thomas and Bendall³¹ which may be used to refine a powder diffraction profile containing up to three phases. This program has already been successfully employed to examine Na₂UCl₆ containing contaminating NaCl³² and also UO₂DAsO₄·4D₂O

† *Non-S.I. units employed:* atm = 101 325 Pa, eV ≈ 1.60 × 10⁻¹⁹ J.

Table 1. Final parameters for $\text{DNb}_6\text{I}_{11}$ at room temperature in space group $P2_1cn$ when all atoms were allowed to refine freely. Estimated standard deviations (e.s.d.s) are given in parentheses

Atom	x	y	z	Atom	x	y	z
D	0.006(9)	-0.006(4)	0.017(6)	I(2)	0.038(10)	0.103(5)	-0.238(5)
Nb(1)	0.092(8)	0.112(3)	-0.042(4)	I(2A)	-0.023(9)	-0.103(5)	0.217(5)
Nb(1A)	-0.117(9)	-0.010(3)	0.021(5)	I(3)	-0.127(8)	0.199(4)	0.022(5)
Nb(2)	0.126(8)	-0.050(4)	0.085(5)	I(3A)	0.059(9)	-0.223(5)	-0.016(5)
Nb(2A)	-0.147(8)	0.061(3)	-0.078(4)	I(4)	0.288(9)	0.015(4)	-0.068(6)
Nb(3)	-0.078(7)	0.057(5)	0.119(5)	I(4A)	-0.320(9)	0.020(3)	0.064(6)
Nb(3A)	0.070(8)	-0.048(4)	-0.127(6)	I(5)	-0.174(11)	0.121(5)	0.312(6)
I(1)	0.1594	0.112(5)	0.171(6)	I(5A)	0.166(11)	-0.133(5)	-0.298(6)
I(1A)	-0.153(7)	-0.124(6)	-0.189(5)	I(6)	0.221(10)	0.266(4)	-0.066(4)

$B(\text{D}) = 2.6(1.5)$, $B(\text{Nb}) = 0.4(4)$, $B(\text{I}) = 0.6(4)$ Å²; $R_1 = 9.2$, $R_p = 17.8$, $R_{wp} = 12.9$, $R_E = 10.6\%$ (all R factors are defined in ref. 28); $a = 11.293(2)$, $b = 15.440(2)$, $c = 13.453(2)$ Å.

Table 2. Bond distances (Å) in $\text{DNb}_6\text{I}_{11}$ for refinement A where all atoms were allowed to move freely; and refinement B where the Nb and I atoms were fixed at the positions calculated from linear interpolation between the parameters determined by X-ray diffraction for the high- and low-temperature forms (see ref. 17). E.s.d.s are given in parentheses

	A	B		A	B
Nb(1)-D	2.21(10)	2.08(6)	Nb(1)-I(1)	2.98(10)	2.87
Nb(1A)-D	2.02(12)	2.04(6)	Nb(1A)-I(1A)	2.89(10)	2.86
Nb(2)-D	1.77(12)	1.86(6)	Nb(1)-I(2)	2.71(9)	2.88
Nb(2A)-D	2.40(12)	2.28(6)	Nb(1A)-I(2A)	2.84(10)	2.88
Nb(3)-D	1.93(11)	1.82(6)	Nb(1)-I(3)	2.95(12)	2.85
Nb(3A)-D	2.18(10)	2.28(6)	Nb(1A)-I(3A)	2.80(12)	2.85
Average	2.09	2.06	Nb(1)-I(4)	2.70(12)	2.86
			Nb(1A)-I(4A)	3.01(12)	2.88
Nb(1)-Nb(2)	3.05(8)	2.90	Nb(2)-I(1)	2.79(10)	2.89
Nb(1A)-Nb(2A)	2.85(7)	2.89	Nb(2A)-I(1A)	3.24(10)	2.92
Nb(1)-Nb(3)	3.02(10)	2.96	Nb(2)-I(2A)	2.59(11)	2.86
Nb(1A)-Nb(3A)	3.02(11)	2.97	Nb(2A)-I(2)	3.08(12)	2.82
Nb(2)-Nb(3)	2.88(11)	2.92	Nb(2)-I(3A)	3.10(10)	2.90
Nb(2A)-Nb(3A)	3.07(12)	2.94	Nb(2A)-I(3)	2.53(8)	2.90
Nb(1)-Nb(2A)	2.85(13)	2.77	Nb(2)-I(4)	2.93(11)	2.84
Nb(1A)-Nb(2)	2.98(13)	2.97	Nb(2A)-I(4A)	2.82(12)	2.85
Nb(1)-Nb(3A)	2.74(8)	2.87	Nb(3)-I(1)	2.91(8)	2.87
Nb(1A)-Nb(3)	2.80(9)	2.74	Nb(3A)-I(1A)	2.91(12)	2.87
Nb(2)-Nb(3A)	2.92(9)	2.76	Nb(3)-I(2A)	2.88(10)	2.87
Nb(2A)-Nb(3)	2.76(9)	2.96	Nb(3A)-I(2)	2.81(10)	2.88
Average	2.91	2.89	Nb(3)-I(3)	2.61(9)	2.86
			Nb(3A)-I(3A)	3.10(10)	2.86
Nb(1)-I(6)	2.82(10)	2.89	Nb(3)-I(4A)	2.90(13)	2.87
Nb(1A)-I(6)	2.84(12)	2.90	Nb(3A)-I(4)	2.77(13)	2.86
Nb(2)-I(5)	2.89(13)	2.92	Average	2.87	2.87
Nb(2A)-I(5A)	2.92(13)	2.96			
Nb(3)-I(5)	2.99(11)	2.91			
Nb(3A)-I(5A)	2.86(11)	2.91			
Average	2.89	2.92			

at 4 K in the presence of ice.³³ Two small regions, where an electrical disturbance had obviously affected the counters, were excluded from the pattern. A total of 328 overlapping reflections contributed to the useful data, including 10 for $\beta\text{-NbD}_{0.7}$ whose structure was modelled in space group $Pnmm$ using the parameters deduced by Somenkov *et al.*³⁴ from powder neutron diffraction.

At room temperature, $\text{DNb}_6\text{I}_{11}$ is in the low-temperature form in space group $P2_1cn$. A description of the structure requires 18 crystallographically distinct atoms, all in the general position 4a (x, y, z). A refinement was performed varying 53 independent atomic positional parameters [the x parameter of I(1) being kept fixed to define the origin], three isotropic thermal parameters for D, Nb, and I respect-

ively, in addition to the normal scale factor, an effective scale factor for $\text{NbD}_{0.7}$, the zero-point, half-width parameters, lattice parameters, and an asymmetric parameter applied below 30° in 2θ . The refinement converged to give the parameters shown in Table 1. Due to the uncertainty in the exact neutron wavelength used, bond lengths were calculated (Table 2) using the lattice parameters estimated from the single-crystal X-ray study, *i.e.* $a = 11.328(5)$, $b = 15.495(8)$, and $c = 13.465(7)$ Å.¹⁷ The observed and calculated profiles are shown in Figure 1. The contaminating minor phase $\beta\text{-NbD}_{0.7}$ appears to have been well accounted for in the refinement. Figure 2 shows the $[\text{DNb}_6\text{I}_8]^{3+}$ cluster.

The results suggest that the D atom in $\text{DNb}_6\text{I}_{11}$ is displaced by 0.37(11) Å away from the centre of gravity of the cage of

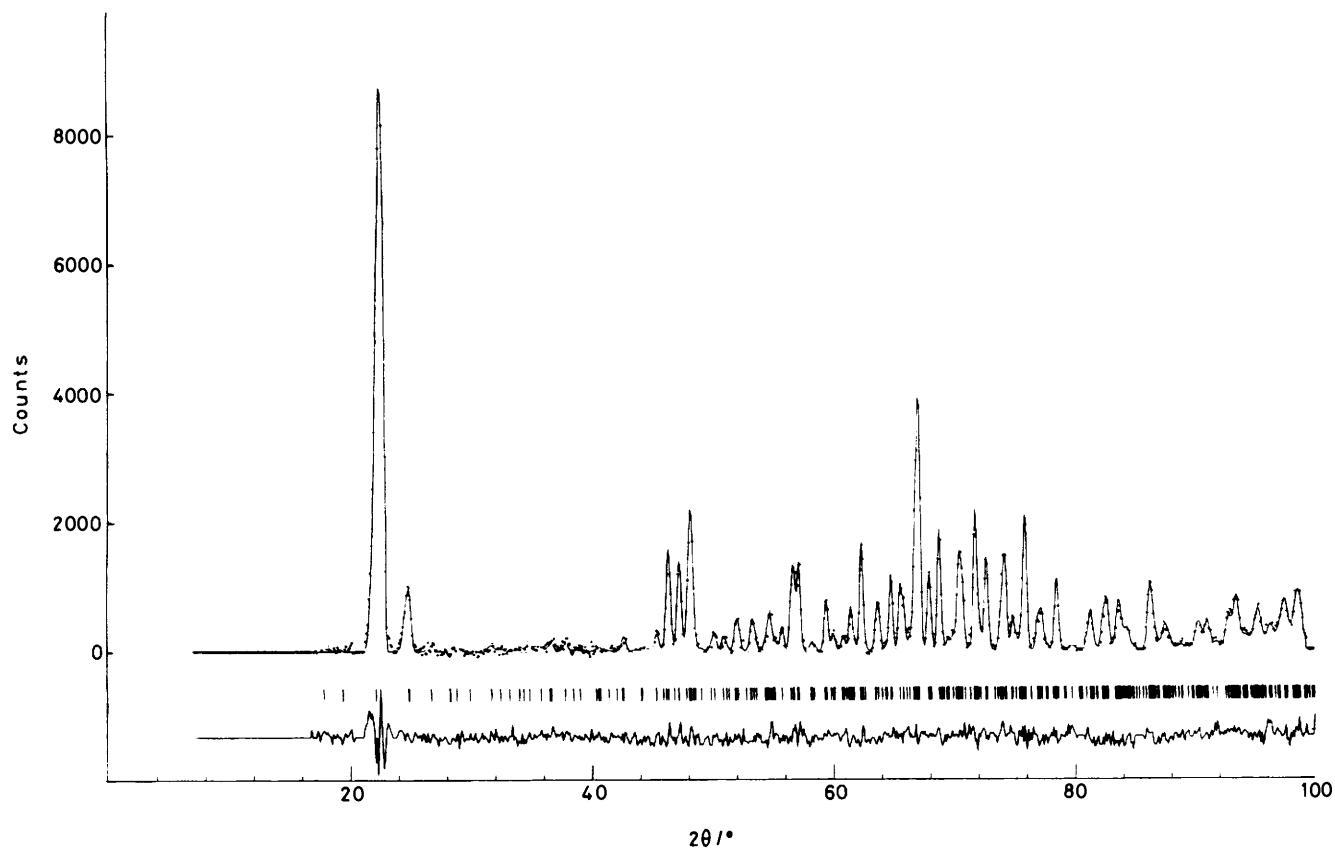


Figure 1. Observed (points), calculated (full curve), and difference powder neutron-diffraction profiles for $\text{DNb}_6\text{I}_{11}$ at room temperature obtained on PANDA at a wavelength of 2.41 \AA

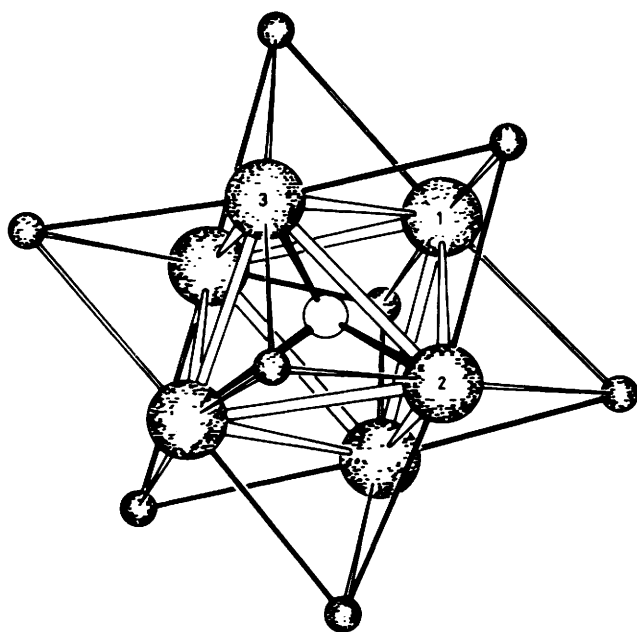


Figure 2. The $[\text{DNb}_6\text{I}_{11}]^{3+}$ cluster showing the three shortest D-Nb bonds

niobium atoms, predominantly towards Nb(2) and the edge of the Nb_6 octahedron joining Nb(3) and Nb(2).

Table 2 gives the bond lengths found in $\text{DNb}_6\text{I}_{11}$ calculated

both from the neutron refinement and also using the *X*-ray determined atom positions. The latter were obtained (at room temperature) by linear interpolation between the positions of the atoms well above and well below the second-order transition, as described by Imoto and Simon.¹⁷ The discrepancies between the two sets of values are mainly within a value of 2σ as estimated from the neutron refinement, but some are between 2 and 3σ . The worst discrepancies occur for the Nb-I distances for the iodine atoms on the faces of the octahedral niobium cage, and for two of these the values differ by an amount almost as large as the observed displacement of D from the centre of the cage, *i.e.* Nb(2A)-I(3) (-0.37 \AA) and Nb(2A)-I(1A) (0.32 \AA). The average discrepancy on the other hand is $\pm 0.12 \text{ \AA}$. The *X*-ray study¹⁷ shows that some of the iodine atoms undergo a marked thermal anisotropy. Our neutron-diffraction data, however, are such that only a very simple isotropic description is possible. The effect of this simplification will be to increase the differences between the neutron and *X*-ray bond lengths as the inadequacies of the description of the thermal motion are partially compensated for by atom shifts. Assuming the maximum difference observed in the heavy-atom bond distances, the deuterium could be very close to the centre of the niobium cage.

An alternative approach to the refinement is to fix the Nb and I atoms at the positions obtained by interpolation from the *X*-ray study. As it is not possible accurately to estimate the thermal parameters by interpolation, these were refined (again isotropically) together with the D positional and thermal parameters. A deuterium displacement of $0.32(6) \text{ \AA}$ is found again towards the Nb(2)-Nb(3) edge of the octahedron. The R_w was 14.4% and R_1 12.1% . The *R* factors, higher than

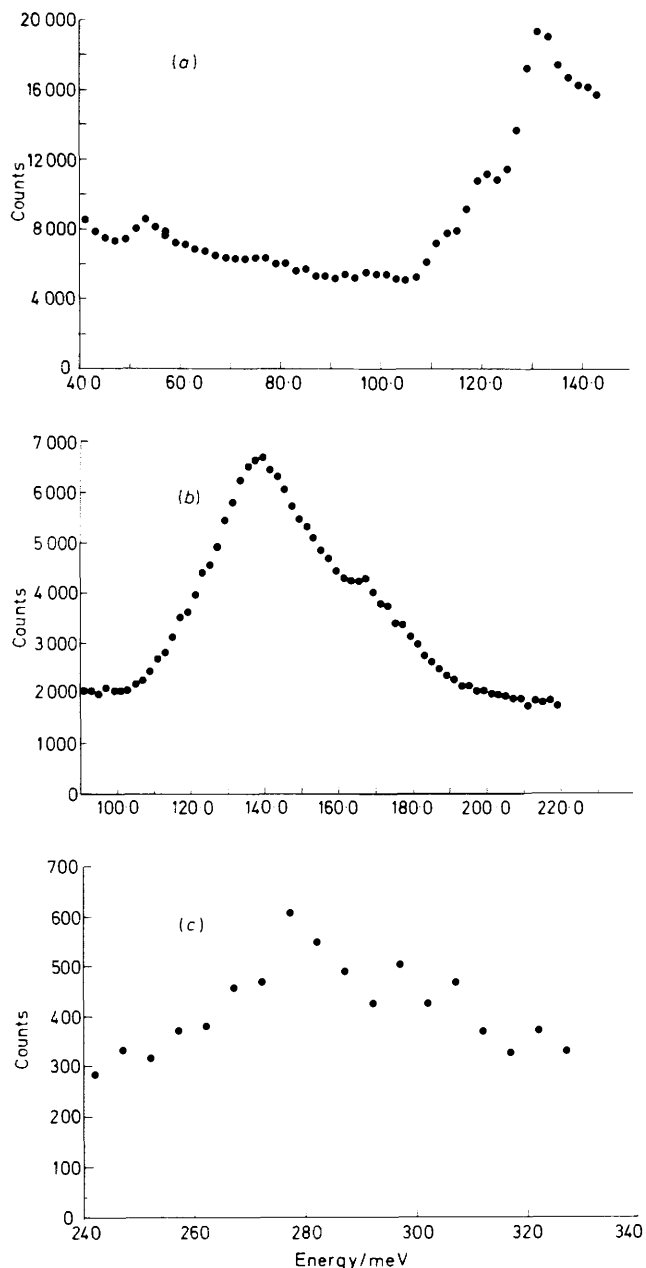


Figure 3. Observed neutron inelastic scattering spectrum of $\text{HNb}_6\text{I}_{11}$ on IN1B using the 200 (a), 220 (b), and 311 (c) planes of the copper monochromator

those given in Table 1, are consistent with the argument above that, when allowed to move, the Nb and I atoms are displaced to some extent to compensate for inadequacies in the simple isotropic vibrational model.

Finally, refinements were attempted with the deuterium atom constrained to the centre of the niobium cage. These produced slightly worse fits to the data, e.g. $R_{wp} = 14.5\%$, for the model with X-ray heavy-atom positions. In addition, the thermal parameters of deuterium increased to $4.1(1.0) \text{ \AA}^2$. The above refinements suggest that the model with the hydrogen atom displaced somewhat from the centre of the niobium cage is the more accurate description of the structure.

Neutron Inelastic Scattering Spectra.—The observed spectra for $\text{HNb}_6\text{I}_{11}$ are illustrated in Figure 3. A strong mode of

about 135 meV is observed for $\text{HNb}_6\text{I}_{11}$ with an overtone just below 280 meV which is assigned to the Nb–H stretch. There is no comparable peak for Nb_6I_{11} in this energy region and only a very weak feature for $\text{DNb}_6\text{I}_{11}$ which is assumed to arise from the small hydrogen content in the deuterium used for the sample preparation. A small peak at ca. 95 meV can be detected in the spectrum of $\text{DNb}_6\text{I}_{11}$ and this band, which is $\approx 1/\sqrt{2}$ the energy of the strong mode in $\text{HNb}_6\text{I}_{11}$, must be the analogous deuterium mode. For $[\text{HRu}_6(\text{CO})_{18}]^-$ and $[\text{DRu}_6(\text{CO})_{18}]^-$ the metal–interstitial hydrogen stretching absorptions are observed at somewhat lower energy, 825 and 600 cm^{-1} (102 and 74 meV) respectively, in the i.r. spectrum.³⁵

With an energy resolution $\Delta E/E$ of the order of 10% for the spectrometer,³⁶ it is clear that the peak at 135 meV in the spectrum of $\text{HNb}_6\text{I}_{11}$ is broad and some structure is observable using the Cu 200 monochromator, although there may be a small contribution from the β -niobium hydride impurity which has two peaks centred at about 120 and 160 meV.³⁷

For zirconium hydride a peak is observed in the neutron inelastic scattering spectrum at about 139 meV which is considerably broadened from that expected of a single Einstein mode by means of hydrogen interactions up to second nearest hydrogen neighbours.³⁸ Such hydrogen interactions would not be expected in $\text{HNb}_6\text{I}_{11}$ where the nearest-neighbour hydrogens occur at a large distance of 8.69 Å. The observed broadening, therefore, probably results from the different strengths of the various Nb–H interactions which are characterized by the displacement of the hydrogen atom from the centre of the niobium cage.

Conclusions

The neutron inelastic scattering studies are compatible with the conclusions from powder diffraction which suggest that the interstitial hydrogen atom in $\text{HNb}_6\text{I}_{11}$ is displaced a small amount from the centre of gravity of the niobium cage. The size of this displacement, which is predominantly towards the Nb(2)–Nb(3) edge of the octahedron, calls into question the assumption of a single hydrogen site at the centre of the cage in the high-temperature phase of this compound. Further studies with high-resolution neutron diffraction and inelastic scattering spectroscopy may clarify this point.

References

- 1 H. Schäfer and H. G. Schnering, *Angew. Chem.*, 1964, **76**, 833.
- 2 D. L. Kepert and K. Vrieze, 'Halogen Chemistry,' ed. V. Gutman, Academic Press, London, 1967, vol. 3, p. 1.
- 3 D. L. Kepert and K. Vrieze, 'Comprehensive Inorganic Chemistry,' ed. J. C. Bailar, Pergamon Press, Oxford, 1973, vol. 4, p. 197.
- 4 F. A. Cotton and T. E. Haas, *Inorg. Chem.*, 1964, **3**, 10.
- 5 H. Schäfer, H. G. Schnering, K. J. Niehues, and H. G. Nieder-Vahrenholtz, *J. Less-Common Met.*, 1965, **9**, 95.
- 6 A. Simon, H. G. Schnering, H. Wöhrle, and H. Schäfer, *Z. Anorg. Allg. Chem.*, 1965, **339**, 155.
- 7 D. Bauer, H. G. Schnering, and H. Schäfer, *J. Less-Common Met.*, 1965, **8**, 388.
- 8 R. Siepmann, H. G. von Schnering, and H. Schäfer, *Angew. Chem. Int. Ed. Engl.*, 1967, **6**, 637.
- 9 D. Bauer and H. G. von Schnering, *Z. Anorg. Allg. Chem.*, 1968, **361**, 259.
- 10 B. Spreckelmeyer, *Z. Anorg. Allg. Chem.*, 1968, **358**, 147.
- 11 H. Schäfer, H. G. von Schnering, J. Tillack, F. Kuhn, H. Wöhrle, and H. Baumann, *Z. Anorg. Allg. Chem.*, 1967, **353**, 281.
- 12 H. Schäfer and R. Siepmann, *Z. Anorg. Allg. Chem.*, 1968, **357**, 273.
- 13 F. A. Cotton, R. M. Wing, and R. A. Zimmermann, *Inorg. Chem.*, 1967, **6**, 11.
- 14 H. Schäfer, H. G. von Schnering, A. Simon, D. Giegling, D.

- Bauer, R. Siepmann, and B. Spreckelmeyer, *J. Less-Common Met.*, 1965, **10**, 154.
- 15 L. R. Bateman, J. F. Blount, and L. F. Dahl, *J. Am. Chem. Soc.*, 1966, **88**, 1082.
- 16 A. Simon, H. G. von Schnering, and H. Schäfer, *Z. Anorg. Allg. Chem.*, 1967, **335**, 295.
- 17 H. Imoto and A. Simon, *Inorg. Chem.*, 1982, **21**, 308.
- 18 A. Simon, *Z. Anorg. Allg. Chem.*, 1967, **355**, 311.
- 19 F. Dübler, H. Müller, and Ch. Opitz, *Chem. Phys. Lett.*, 1982, **88**, 467.
- 20 A. Simon, *Bull. Soc. Chim., Fr.* in the press.
- 21 H. Imoto and J. D. Corbett, *Inorg. Chem.*, 1980, **19**, 1241.
- 22 A. W. Struss and J. D. Corbett, *Inorg. Chem.*, 1977, **16**, 340.
- 23 J. D. Corbett, in 'Intercalation Chemistry,' eds. M. S. Whittingham and A. J. Jacobson, Academic Press, New York, 1982, p. 361.
- 24 J. J. Finley, H. Nohl, E. E. Vogel, H. Imoto, R. E. Camley, V. Zevin, O. K. Andersen, and A. Simon, *Phys. Rev. Lett.*, 1981, **46**, 1472.
- 25 J. J. Finley, R. E. Camley, E. E. Vogel, V. Zevin, and E. Gmelin, *Phys. Rev. B*, 1981, **24**, 1323.
- 26 D. W. Hart, R. G. Teller, C. Wei, R. Bau, G. Longoni, S. Campanella, P. Chini, and T. F. Koetzle, *Angew. Chem. Int. Ed. Engl.*, 1979, **18**, 80.
- 27 R. W. Broach, L. F. Dahl, G. Longoni, P. Chini, A. J. Schultz, and J. M. Williams, *Adv. Chem. Ser.*, 1978, **167**, 93.
- 28 H. M. Rietveld, *J. Appl. Crystallogr.*, 1969, **2**, 65.
- 29 L. Koester and H. Rauch, IAEA report 2517/RB, 1981.
- 30 W. M. Mueller, J. P. Blackledge, and G. G. Libowitz, 'Metal Hydrides,' Interscience, New York, 1968.
- 31 M. W. Thomas and P. J. Bendall, *Acta Crystallogr., Sect. A*, 1978, **34**, S351.
- 32 P. J. Bendall, A. N. Fitch, and B. E. F. Fender, *J. Appl. Crystallogr.*, 1983, **16**, 164.
- 33 A. N. Fitch, A. F. Wright, and B. E. F. Fender, *Acta Crystallogr., Sect., B*, 1982, **38**, 2546.
- 34 V. A. Somenkov, A. V. Gurskaya, M. G. Zemlyanov, M. E. Kost, N. A. Chernoplekov, and A. A. Cherkhov, *Soc. Phys.-Solid State*, 1968, **10**, 1076.
- 35 I. A. Oxtton and S. F. A. Kettle, *J. Chem. Soc., Chem. Commun.*, 1979, 687.
- 36 H. Jobic, R. E. Ghosh, and A. Renouprez, *J. Chem. Phys.*, 1981, **75**, 4025.
- 37 K. Brand, *Atomkernenergie*, 1971, **17**, 113.
- 38 E. L. Slaggie, *J. Phys. Chem. Solids*, 1968, **29**, 923.

Received 28th February 1983; Paper 3/325